09

Evolution of Structural and Spectral Characteristics of $Lu_{0.99-x}Sm_xEu_{0.01}BO_3$ orthoborates

© S.Z. Shmurak, V.V. Kedrov, A.P. Kiselev, T.N. Fursova, I.I. Zver'kova

Osipyan Institute of Solid State Physics RAS,
Chernogolovka, Russia

E-mail: shmurak@issp.ac.ru

Received October 18, 2022
Revised October 18, 2022
Accepted October 19, 2022

The structure, IR absorption and luminescence spectra, and morphology of $Lu_{0.99-x}Sm_xEu_{0.01}BO_3$ ($0 \le x \le 0.99$) orthoborates synthesized at 970°C were studied. With an increase in the Sm^{3+} concentration, a successive change of five structural states is observed: calcite ($0 \le x \le 0.1$) → calcite + vaterite ($0.1 < x < 0.3$) → vaterite ($0.3 \le x \le 0.95$) → vaterite + a triclinic phase ($0.95 < x \le 0.98$) → a triclinic phase ($0.98 < x \le 1$). A wide range of Sm^{3+}, concentrations at which the vaterite phase ($0.3 \le x \le 0.95$) exists and a very narrow region of triclinic phase formation ($0.98 < x \le 1$) are important distinctive features of this system. Correspondence between the structure and spectral characteristics of these compounds was established. It is shown that the vaterite phase appears in the bulk of the microcrystals of the samples that have a calcite structure.

Keywords: rare earth orthoborates, crystal structure, X-ray diffraction analysis, IR-spectroscopy, luminescence spectra.

DOI: 10.21883/PSS.2023.02.55417.504

1. Introduction

Borates, that contain rare-earth ions are effective luminophores and can be used as materials for color displays, X-ray luminophores, light sources based on light-emitting diodes [1–5]. Spectral characteristics of these compounds are dependent on both the electron structure of optically active luminescence centers and the crystal structure matrix where they are located. For example, Eu^{3+} ions in borates with a structure of calcite, $Me(BO_3):Eu$, $Me = Lu, In$ and vaterite, $Re(BO_3):Eu$, $Re =$ Lu, Tb, Eu, Gd, Y are characterized by orange and red luminescence, respectively [3,6–9]. The luminescence intensity at resonance excitation ($\lambda_{ex} = 394$ nm) of Eu^{3+} ions contained in borates with a vaterite structure is more than an order of magnitude higher than that in the samples with a calcite structure. Therefore, the change in structural state of compounds containing optically active rare earth ions allows for changing their spectral characteristics in a targeted manner.

As known, lutetium borate ($LuBO_3$) has two stable structural modifications: vaterite formed during synthesis of $LuBO_3$ at $T = 750-850$°C, and calcite formed at $T = 970-1100$°C [10–12]. $ReBO_3$ orthoborates ($Re =$ Eu, Gd, Tb, Dy, Y) and ($InBO_3$) have one structural modification: $ReBO_3$ — vaterite, $InBO_3$ — calcite [10–15]. $LaBO_3$ and $PrBO_3$ compounds have two phase states. Low-temperature phase of these compounds is the orthorhombic phase−aragonite (sp. gr. $Pnam$). At $T = 1488$°C $LaBO_3$ transits to the high-temperature monoclinic phase (sp. gr. $P2_1/m$), and $PrBO_3$ at $T = 1500$°C transits to the triclinic phase (sp. gr. P-1) [16–21].

It is worth to note, that La^{3+} ions in the aragonite structure are surrounded by nine oxygen ions, while boron ions have a trigonal coordination by oxygen [18–21]. Lu^{3+} ions in the calcite structure, e.g. in $LuBO_3$, are surrounded by six oxygen ions, while boron atoms have the same trigonal coordination by oxygen, as that in aragonite, — $(BO_3)^{3-}$ [22]. At the same time, Lu^{3+} ions in the vaterite structure are surrounded by eight oxygen ions, while three boron atoms with a tetrahedral environment by oxygen make up a group $(B_3O_9)^{9-}$ in the form of a three-dimensional ring [23,24].

In [8,25–28] structural and spectral characteristics of $Lu_{0.98-x}In_xEu_{0.02}BO_3$, $Lu_{0.99-x}Re_xEu_{0.01}BO_3$ ($Re =$ Eu, Gd, Tb, Y), $La_{0.98-x}Lu_xEu_{0.02}BO_3$ and $Pr_{0.99-x}Lu_xEu_{0.01}BO_3$ orthoborates are investigated. In the $Lu_{0.98-x}In_xEu_{0.02}BO_3$ orthoborate synthesized at $T = 780$°C (the temperature of existence of the low-temperature $LuBO_3$ vaterite), with increase in concentration of In the following structural modifications sequence (SMS) is observed: vaterite ($0 \le x < 0.03$) → vaterite + calcite ($0.03 \le x < 0.1$) → calcite ($x \le 0.1$). In $Lu_{0.99-x}Re_xEu_{0.01}BO_3$ compounds ($Re =$ Eu, Gd, Tb, Y), synthesized at $T = 970$°C (the temperature of existence of the $LuBO_3$ calcite phase), with increase in concentration of Re a successive change of structural states is observed (Table 1): calcite ($0 \le x \le 0.05-0.1$) → calcite + vaterite ($0.05-0.1 < x \le 0.1-0.25$) → vaterite ($x > 0.1-0.25$). Since at 970°C the $LaBO_3$ orthoborate has a structure of aragonite, and the $LuBO_3$ has a structure of calcite, then it could be expected that in the $La_{0.98-x}Lu_xEu_{0.02}BO_3$ compounds synthesized at 970°C with an increase in x

Table 1. Regions of *Re* concentrations where certain structural states of $Lu_{1-x}Re_xBO_3$ orthoborates exist (*Re* = Gd, Eu, Tb and Y)

Compound	Values of x at which the given structures exist		
	Calcite ($R\bar{3}c$)	Calcite ($R\bar{3}c$) + Vaterite ($C2/c$)	Vaterite ($C2/c$)
$Lu_{0.99-x}Gd_xEu_{0.01}BO_3$	$0 \le x \le 0.05$	$0.05 < x \le 0.1$	$x > 0.1$
$Lu_{1-x}Eu_xBO_3$	$0 \le x \le 0.07$	$0.07 < x < 0.2$	$x \ge 0.2$
$Lu_{0.99-x}Tb_xEu_{0.01}BO_3$	$0 \le x \le 0.09$	$0.09 < x < 0.2$	$x \ge 0.2$
$Lu_{0.99-x}Y_xEu_{0.01}BO_3$	$0 \le x \le 0.10$	$0.1 < x < 0.25$	$x \ge 0.25$

the following SMS will be observed: aragonite → aragonite + calcite → calcite. However, as it is shown in [27], another sequence of structural states is observed in these samples: aragonite $(0 \le x < 0.15)$ → aragonite + vaterite $(0.15 \le x \le 0.8)$ → vaterite $(0.8 < x < 0.88)$ → vaterite + calcite $(0.88 \le x < 0.93)$ → calcite $(0.93 \le x \le 0.98)$. The same sequence of structural states change is also observed in $Pr_{0.99-x}Lu_xEu_{0.01}BO_3$ orthoborates. The only difference is that in these samples the single-phase vaterite is observed in a wider range of Lu^{3+} concentrations: $(0.6 < x \le 0.8)$ [28].

It is important to note, that in $Lu_{0.98-x}In_xEu_{0.02}BO_3$ synthesized at $T = 780°C$, the single-phase calcite is formed even at an In concentration of 10 at.%, while in samples of $Lu_{0.99-x}Re_xEu_{0.01}BO_3$ (*Re* = Eu, Gd, Tb, Y) synthesized at $T = 970°C$, the vaterite is formed at *Re* concentrations of 10–25 at.% (Table 1). At the same time, in $La_{0.98-x}Lu_xEu_{0.02}$ BO_3 and $Pr_{0.99-x}Lu_xEu_{0.01}BO_3$ compounds synthesized at $T = 970°C$, calcite is only formed at concentrations of Lu^{3+} 93 and 95 at.%, respectively.

As it was noted before, in [8,25–29] structural and spectral characteristics were investigated for $LuBO_3$(Eu) compounds and borates of one of the following structures: calcite, vaterite, or aragonite. It seems reasonable to carry out such studies of $LuBO_3$(Eu) compounds and a borate with a structural modification other than above-listed structures. These requirements are met by $SmBO_3$, which has a triclinic structure at $T = 970°C$ and transits to a vaterite structure at a temperature of $T = 1065–1150°C$ (according to different studies) [10,30–32].

In $Lu_{1-x}Sm_xBO_3$(Eu) compounds synthesized at $T = 970°C$ (the temperature of existence of the $LuBO_3$ calcite phase and the $SmBO_3$ triclinic phase), with increase in x the following structural modifications sequence could be expected: calcite → calcite + triclinic phase → triclinic phase. However, as it is shown in this work, another, more complicated sequence of structural states is observed.

In this work we performed studies of changes in the structure, IR-spectra, luminescence spectra, and luminescence excitation spectra of $La_{0.99-x}Sm_xEu_{0.01}BO_3$ orthoborates at $0 \le x \le 0.99$. The correspondence between structure and spectral characteristics of these compounds is found. The ions Eu^{3+}, like in our previous research, were used as optically active and structure-sensitive labels in amounts not affecting the structural transformations of orthoborates.

2. Experimental procedures

2.1. Synthesis of samples

Samples of polycrystalline powders of orthoborates of the $La_{0.99-x}Sm_xEu_{0.01}BO_3$ compositions were obtained by interaction of oxides of rare earth elements with a melt of potassium tetraborate by the following reaction:

$$(0.99 - x)Lu_2O_3 + xSm_2O_3 + 0.01Eu_2O_3 + K_2B_4O_7 = 2Lu_{0.99-x}Sm_xEu_{0.01}BO_3 + K_2B_2O_4.$$

The amount of potassium tetraborate taken into the reaction provided an excess of the boron-containing reagent relative to the stoichiometric amount by 10–20%. The initial compounds for orthoborate synthesis were potassium tetraborate tetrahydrate $K_2B_4O_7 \cdot 4H_2O$ and calibrated aqueous solutions of nitrates of rare earth elements. All the chemicals used corresponded to the „AR grade“ qualification.

Microcrystalline orthoborate powders were synthesized as follows. A weighed amount of potassium tetraborate tetrahydrate was placed in a ceramic round-bottomed cup, stoichiometric amounts of aqueous solutions of rare earth nitrates, taken in the required ratio, were added and thoroughly mixed. The resulting aqueous suspension was heated on a tile and water was distilled at low boiling. The resulting solid product was annealed at a temperature of 550°C for 20 min to remove water and nitrate decomposition products, after which it was thoroughly ground in an agate mortar. The obtained powder was transferred into a ceramic crucible and subjected to high-temperature annealing at $T = 970°C$ for 2 h. The annealing product was treated with aqueous solution of hydrochloric acid with a concentration of 5 wt.% for 0.2 h while constantly mixing on a magnetic mixer. Orthoborate polycrystals were isolated by filtering the obtained aqueous suspension, followed by washing with water, alcohol, and product drying on a filter. The obtained powders of polycrystals of orthoborates were finally dried in the air at $T = 200°C$ for 0.5 h.

2.2. Research methods

X-ray diffraction studies were performed using a Rigaku SmartLab SE diffractometer with CuK_α-radiation,

Table 2. Content of calcite (C), vaterite (V), and triclinic (Tr) phases in $Lu_{1-x-y}Sm_xEu_yBO_3$ orthoborates

Concentration *Re*, at.%			C, %	V_C, Å^3	V, %	V_V, Å^3	Tr, %	V_{Tr}, Å^3
Lu	Sm	Eu						
99	0	1	100	113.08	0	–	0	–
89	10	1	100	113.89	0	–	0	–
79	20	1	69	114.25	31	106.50	0	–
74	25	1	39	114.19	61	106.39	0	–
69	30	1	0	–	100	106.53	0	–
49	50	1	0	–	100	108.52	0	–
29	70	1	0	–	100	110.79	0	–
9	90	1	0	–	100	113.92	0	–
5	95	0	0	–	100	115.01	0	–
3.5	96.5	0	0	–	44	114.92	56	117.61
2	98	0	0	–	9	114.76	91	117.42
0	100	0	0	–	0	–	100	117.58

Note. V_C — volume of calcite lattice cell ($Z = 6$) reduced to $Z = 2$; V_V — volume of vaterite lattice cell, $Z = 2$; V_{Tr} — volume of triclinic lattice cell ($Z = 4$) reduced to $Z = 2$.

$\lambda = 1.54178$ Å, 40 kV, 35 mA. Angular interval was $2\theta = 10-140°$. Phase analysis of the samples and calculation of lattice parameters were performed using the Match and PowderCell 2.4 programs.

The IR absorption spectra of the samples were measured using a VERTEX 80v Fourier-spectrometer in the spectral range of $400-5000\,cm^{-1}$ with a resolution of $2\,cm^{-1}$. For measurements, the polycrystal powders were ground in an agate mortar, and then were applied in a thin layer onto a polished crystalline substrate of KBr. The sample morphology was studied using a Supra 50VP X-ray microanalyzer with an add-on for EDS INCA (Oxford).

Photoluminescence spectra and luminescence excitation spectra were studied on a unit consisting of a light source — DKSSh-150 lamp, two MDR-4 and MDR-6 monochromators (spectral range 200–1000 nm, dispersion 1.3 nm/mm). Luminescence was recorded by means of a FEU-106 photomultiplier (spectral sensitivity region 200–800 nm) and an amplification system. The MDR-4 monochromator was used to study the samples' luminescence excitation spectra, the MDR-6 monochromator was used to study luminescence spectra.

The spectral and structural characteristics, as well as the morphology of the samples, were studied at room temperature.

3. X-ray diffraction studies

Diffraction patterns for powder samples of $Lu_{0.99-x}Sm_xEu_{0.01}BO_3$ at $0 \le x \le 0.99$ are shown in Fig. 1. Phase composition of the studied compounds and unit cell volumes are shown in Fig. 2, 3 and in Table 2. In the range of concentrations of $0 \le x \le 0.1$ $Lu_{0.99-x}Sm_xEu_{0.01}BO_3$ orthoborates are single-phase with a structure of calcite, sp. gr. $R\bar{3}c$ № 167 (PDF 72-1053), $Z = 6$. In the range of $0.1 < x < 0.3$ the samples are double-phase — they contain calcite and vaterite, sp. gr. $P6_3/mmc$ № 194 (PDF 74-1938), $Z = 2$. In a wide range of concentrations $0.3 \le x \le 0.95$ the samples are single-phase with a vaterite structure. The samples with a composition of $Lu_{1-x}Sm_xBO_3$ at $0.95 < x \le 0.98$ are double-phase — they contain (along with vaterite) the triclinic phase $SmBO_3$, sp. gr. $P(-1)$ № 2 (PDF 88-2007), $Z = 4$. The sample with a composition of $SmBO_3$ is single-phase and has a triclinic structure. It should be noted, that in the range of concentrations of Sm^{3+} 95–100 at.% a fundamental change in the structure of samples is observed (Fig. 1, 2, Table 2). Therefore, to exclude the impact of Eu^{3+} ions on the structure of samples, in this range of concentrations of Sm^{3+} the compounds were not doped with Eu^{3+} ions (Fig. 1, 2, Table 2).

In single-phase samples with calcite structure at $0 \le x \le 0.1$ with increase in concentrations of samarium ions the lattice cell volume increases (Fig. 3, Table 2). This is indicative of the fact that Sm^{3+} ions with an ion radius of 1.00148 Å substitute for Lu^{3+} ions that have smaller ion radius (0.86722 Å) [33]. Maximum possible dissolution of Sm^{3+} ions in the calcite lattice is ~ 10 at.%. Composition of the resulted solid solution is $\sim Lu_{0.89}Sm_{0.1}Eu_{0.01}BO_3$. With further doping the additional samarium is no longer included into the calcite structure, but is spent for the growth of vaterite phase. In the double-phase region (calcite + vaterite) in the range of concentrations of $0.2 \le x < 0.3$ no changes in volumes of lattice cells are observed, only the ratio of calcite and vaterite phases quantities is changed. In single-phase samples with a structure of vaterite at $0.3 \le x \le 0.95$ with an increase in concentration of Sm^{3+} an increase in lattice cell volume is observed, which is indicative of the fact that samarium ions substitute for lutetium ions in the vaterite lattice in $Lu_{0.99-x}Sm_xEu_{0.01}BO_3$ compounds (Fig. 3).

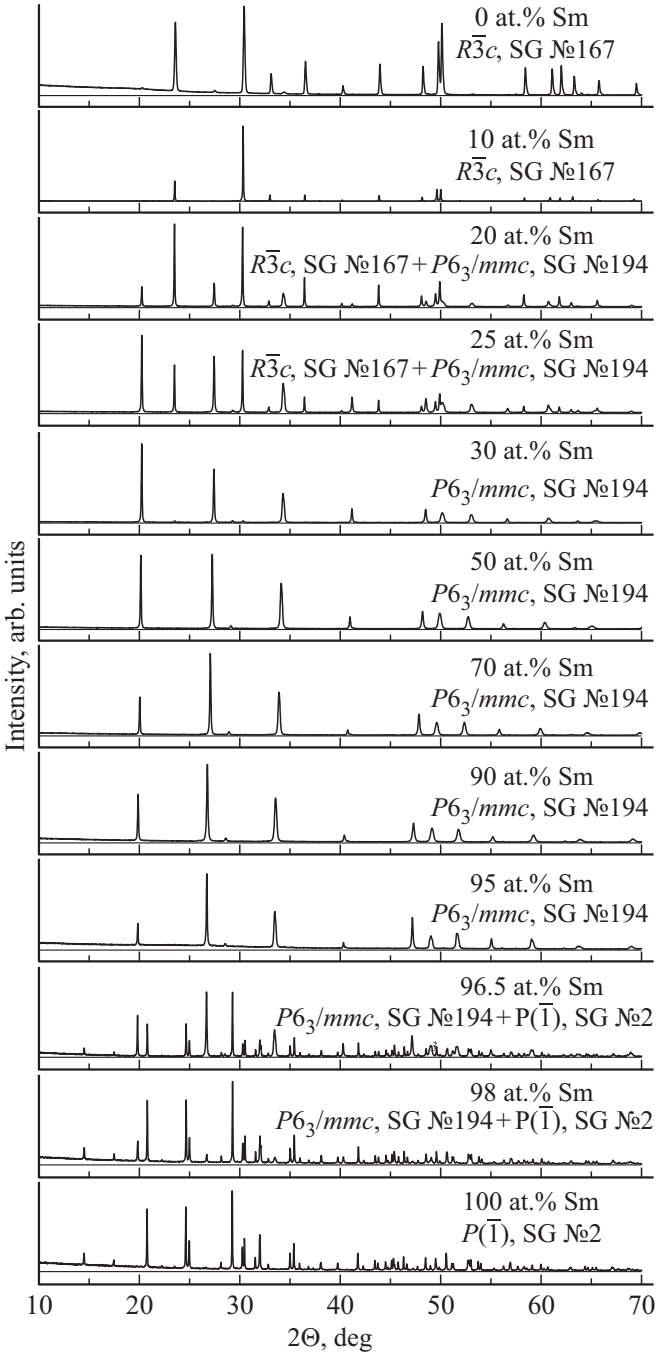

Figure 1. Diffraction patterns for samples of $Lu_{0.99-x}Sm_xEu_{0.01}BO_3$.

Fig. 4 shows the shift of the vaterite diffraction line (100) in single-phase samples at an increase in concentration of the doping addition of samarium from 30 to 95%. The line is shifted toward smaller angles, i.e. larger interplane distances, because the ion radius of Sm^{3+} (1.00148 Å) is greater than the ion radius of Lu^{3+} (0.86722 Å). This shift is correlated with the increase in lattice cell volume of vaterite in $Lu_{0.99-x}Sm_xEu_{0.01}BO_3$ compounds when Lu^{3+} ions are substituted by Sm^{3+} ions.

The approximate composition of the vaterite phase evaluated by the boundary of cell volume change in case of transition from the double-phase region (calcite + vaterite) to the single-phase vaterite, — $Lu_{0.69}Sm_{0.3}Eu_{0.01}BO_3$ (Fig. 3). The approximate composition of the vaterite doped with samarium to the maximum possible extent, which is evaluated by the boundary of cell volume change in case of transition from the vaterite to the double-phase region (vaterite + triclinic phase) meets the following formula: $\sim Lu_{0.05}Sm_{0.95}BO_3$. Thus, the range of compositions with observed single-phase vaterite is from $\sim Lu_{0.69}Sm_{0.3}Eu_{0.01}BO_3$ to $\sim Lu_{0.05}Sm_{0.95}BO_3$. In the double-phase region (vaterite + triclinic phase) at $0.95 < x \leq 0.98$ a change is observed in the ratio of quantities of these two phases and in the case of $SmBO_3$

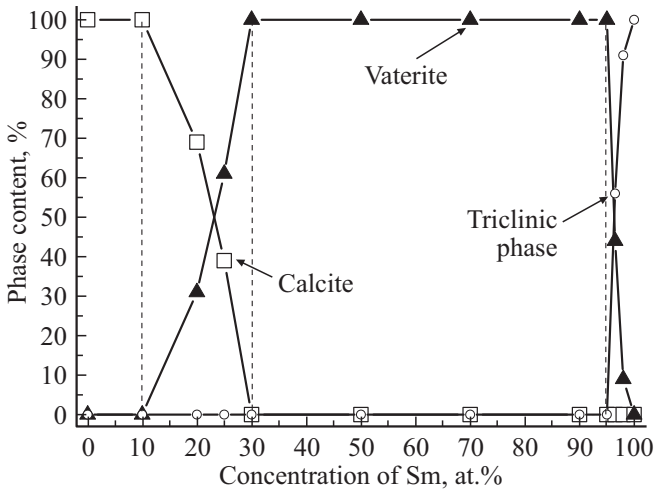

Figure 2. Phase composition of the synthesized samples of $Lu_{0.99-x}Sm_xEu_{0.01}BO_3$ depending on Sm^{3+} concentration in the batch: square — calcite, triangle — vaterite, circle — triclinic phase.

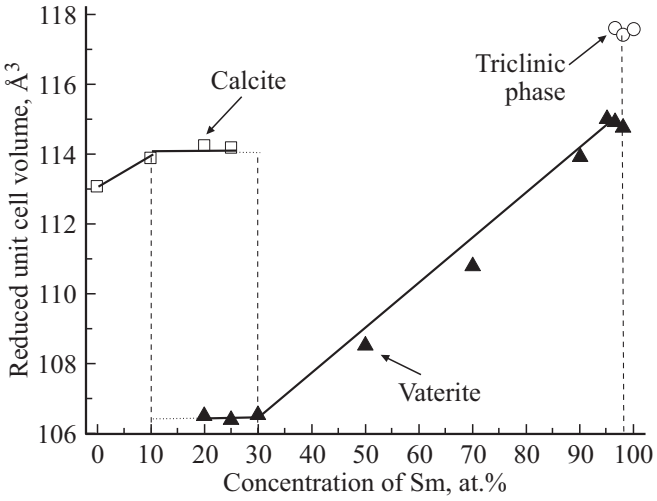

Figure 3. Volumes of lattice cells of $Lu_{0.99-x}Sm_xEu_{0.01}BO_3$ structural modifications reduced to $Z = 2$: square — calcite, triangle — vaterite, circle — triclinic phase.

composition the sample is single-phase with a triclinic structure. Two phase states, i.e. vaterite and triclinic phase, are simultaneously observed in $Lu_{1-x}Sm_xBO_3$ compounds in a very narrow range of Sm^{3+} concentrations: $0.95 < x \leq 0.98$. In an even more limited range of Sm^{3+} concentrations (at $0.98 < x \leq 1$) the sample is single-phase and has a triclinic structure.

Based on results of X-ray diffraction studies a conclusion can be made that in $Lu_{0.99-x}Sm_xEu_{0.01}BO_3$ orthoborates synthesized at $T = 970°C$ (the temperature of existence of the $LuBO_3$ calcite phase and the $SmBO_3$ triclinic phase), with an increase in Sm^{3+} concentration a successive change of five structural states is observed: calcite $(0 \leq x \leq 0.1) \rightarrow$ calcite + vaterite $(0.1 < x < 0.3) \rightarrow$ vaterite $(0.3 \leq x \leq 0.95) \rightarrow$ vaterite + triclinic phase $(0.95 < x \leq 0.98) \rightarrow$ triclinic phase $(0.98 < x \leq 1)$. Thus, regardless of the fact that at 970°C calcite and triclinic phase are equilibrium phases for $LuBO_3$ and $SmBO_3$, at samarium concentrations of 30–95 at.% $Lu_{0.99-x}Sm_xEu_{0.01}BO_3$ orthoborates have a structure of vaterite. This situation is similar to that observed in $Re_{1-x}Lu_xBO_3$(Eu) (Re = La, Pr) compounds synthesized at 970°C (the temperature of existence of the $ReBO_3$ aragonite phase and the $LuBO_3$ calcite phase). With an increase in lutetium concentration the $Re_{1-x}Lu_xBO_3$(Eu) has a structure of aragonite, then vaterite, and, finally, calcite [28,29].

It is important to note that the range of Sm^{3+} concentrations where the vaterite phase exists in $Lu_{0.99-x}Sm_xEu_{0.01}BO_3$ orthoborates synthesized at 970°C is very wide: $0.3 \leq x \leq 0.95$, at the same time, the triclinic phase exists in a very narrow range: $0.98 < x \leq 1$.

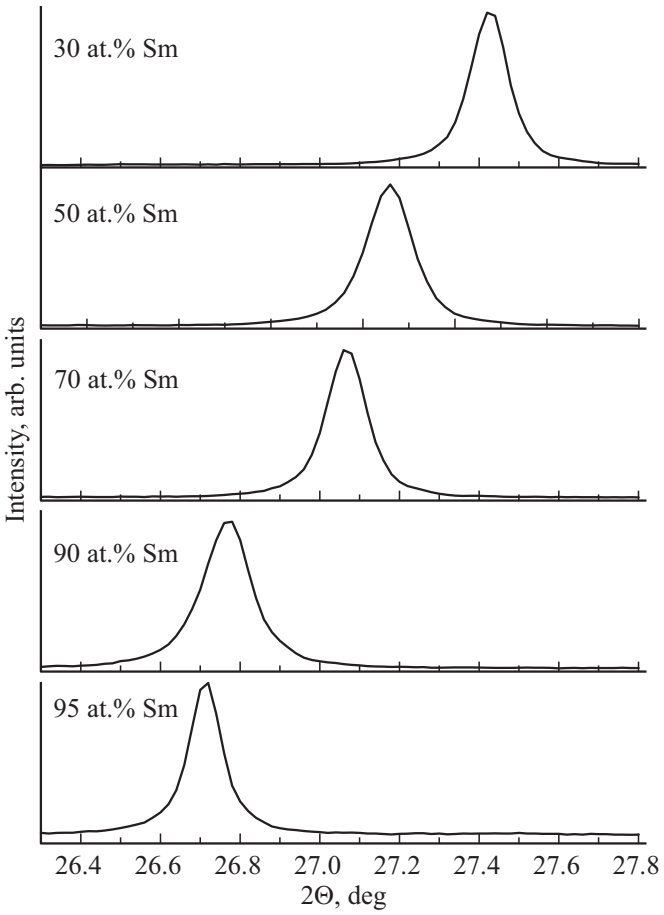

Figure 4. Position of the diffraction peak (100) for single-phase samples (vaterite) of $Lu_{0.99-x}Sm_xEu_{0.01}BO_3$ at $0.3 \leq x \leq 0.95$.

4. Morphology of samples

$Lu_{0.99-x}Sm_xEu_{0.01}BO_3$ orthoborates at $0 \leq x \leq 0.1$, that, according to the X-ray phase analysis data, have a calcite structure (Table 2), contain well edged microcrystals with a size of $\sim 2-8\,\mu$m (Fig. 5, *a*). In the double-phase region $(0.1 < x < 0.3)$ in samples, small microcrystals $(0.5-2\,\mu$m) occurs along with larger microcrystals $(2-5\,\mu$m). According to the X-ray phase analysis data, an increase in concentration of Sm^{3+} ions leads to a decrease in the calcite amount and an increase in the vaterite share (Table 2). With an increase in the share of vaterite phase, the number of small microcrystals $(0.5-2\,\mu$m) grows (Fig. 5, *b, c*). The morphology of samples with a vaterite structure (at $0.3 \leq x \leq 0.95$) (Table 2) changes significantly with an increase in concentration of Sm^{3+} ions (Fig. 5, *c, d, e, f, g*). In the compounds that contain 30 and 50 at.% of samarium small microcrystals $(0.5-2\,\mu$m) are observed together with larger microcrystals with a size of $3-5\,\mu$m (Fig. 5, *c, d*). Samples of $Lu_{0.29}Sm_{0.7}Eu_{0.01}BO_3$ contain shapeless small $(0.5-2\,\mu$m) and larger $(3-5\,\mu$m) microcrystals, which have numerous discontinuities (cracks) (Fig. 5, *e*). In $Lu_{0.09}Sm_{0.9}Eu_{0.01}BO_3$ compounds small microctystals $(0.5-2\,\mu$m) observed, which are grouped in larger buildups with a size of $3-5\,\mu$m (Fig. 5, *f*). This morphology of samples containing 90 at.% of samarium is due most likely to the fact that small microcrystals were formed as a result of destruction of larger microcrystals. Absolutely another morphology is observed in samples of $Lu_{0.05}Sm_{0.95}BO_3$. These samples, that have a structure of vaterite as well, are made up of thin platy microcrystals and separate microcrystals $(3-6\,\mu$m) with numerous cracks (Fig. 5, *g*). The $Lu_{0.035}Sm_{0.965}BO_3$ compounds contain platy microcrystals $0.2 \times 3-5\,\mu$m and microcrystals with a size of $3-5\,\mu$m with numerous discontinuities (cracks), as well as well edged microcrystals with a size of $3-5\,\mu$m (Fig. 5, *h*). Samples of $Lu_{0.02}Sm_{0.98}BO_3$, that contain 44% of vaterite and 56% of triclinic phase and $SmBO_3$ having a triclinic structure (Table 2) are made up of well edged microcrystals, which size is $2-6\,\mu$m (Fig. 5, *k, l*).

Thus, the investigation of morphology of $Lu_{0.99-x}Sm_xEu_{0.01}BO_3$ orthoborates at $0 \leq x \leq 0.99$ has shown that samples of calcite phase ($x = 0.1$) and triclinic phase $SmBO_3$ are made up of well edged microcrystals. For all other compositions the morphology of samples is more complicated and depends on the concentration of samarium.

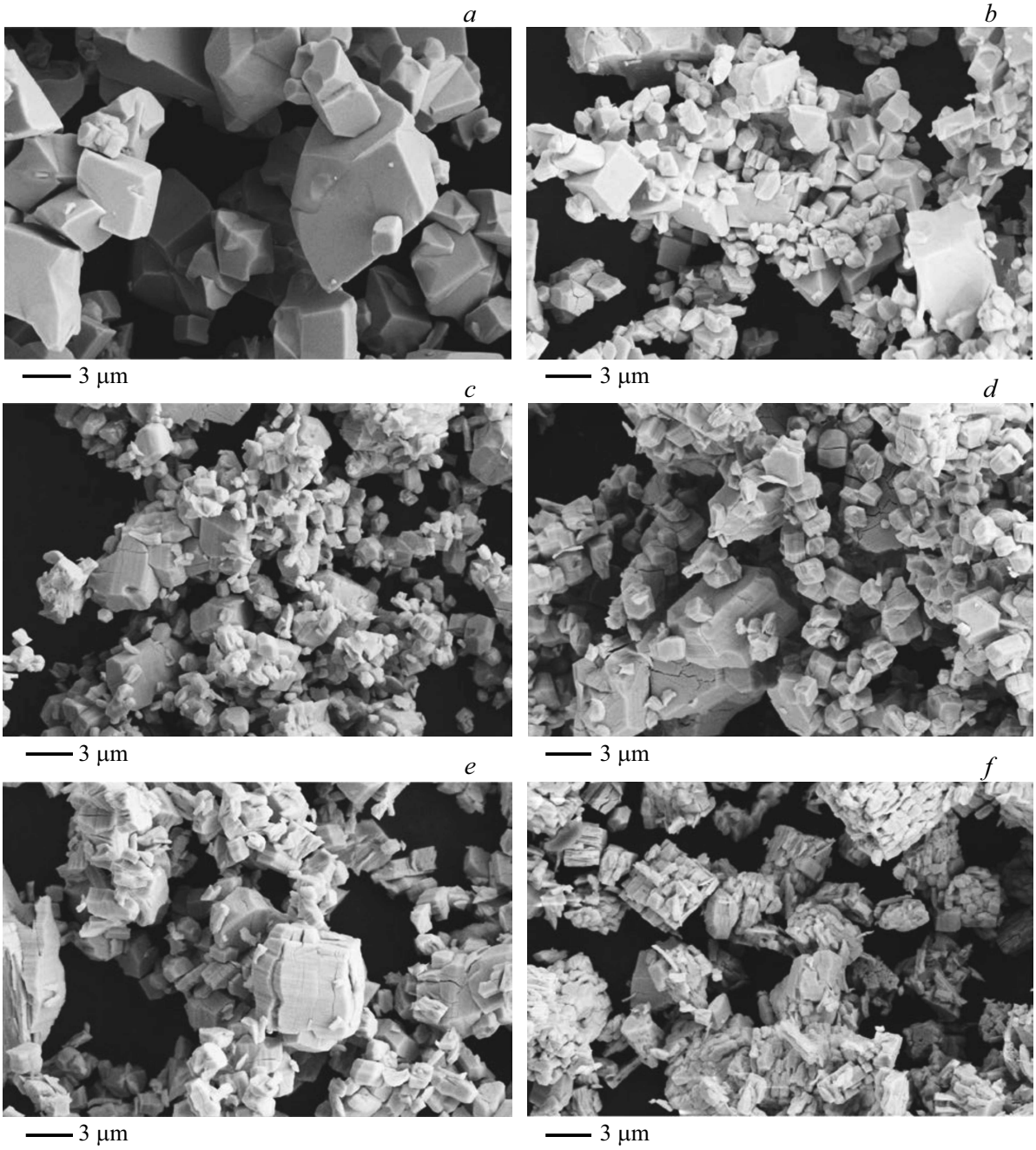

Figure 5. Morphology of samples *a* — $Lu_{0.89}Sm_{0.1}Eu_{0.01}BO_3$; *b* — $Lu_{0.79}Sm_{0.2}Eu_{0.01}BO_3$; *c* — $Lu_{0.69}Sm_{0.3}Eu_{0.01}BO_3$; *d* — $Lu_{0.49}Sm_{0.5}Eu_{0.01}BO_3$; *e* — $Lu_{0.29}Sm_{0.7}Eu_{0.01}BO_3$; *f* — $Lu_{0.09}Sm_{0.9}Eu_{0.01}BO_3$; *g* — $Lu_{0.05}Sm_{0.95}BO_3$; *h* — $Lu_{0.035}Sm_{0.965}BO_3$; *k* — $Lu_{0.02}Sm_{0.98}BO_3$; *l* — $SmBO_3$.

5. Results of IR-spectroscopy

Orthoborates of rare-earth elements with a general formula of $ReBO_3$ (Re = La–Lu) feature a variety of crystal structures, where boron atoms have trigonal (BO_3) or tetrahedral (BO_4) coordination by oxygen. In the first case molecular orbitals of three atoms of oxygen and an atom of boron are in the state of sp^2-hybridization, and in the case of four atoms of oxygen they are in the state of sp^3-hybridization, which have a considerable effect on IR-spectra of rare earth orthoborates. Therefore, the IR-spectroscopy is used as an additional method to identify structures of these compounds.

Fig. 6 shows IR-spectra of absorption for the samples of some investigated compounds of $Lu_{0.99-x}Sm_xEu_{0.01}BO_3$ ($0 \le x \le 0.99$). In the spectrum of the sample of $Lu_{0.99}Eu_{0.01}BO_3$ compound ($x = 0$), which, according to the X-ray phase analysis data (Table 2), has a structure of calcite, absorption bands with maxima at 629, 747, 773, and 1239 cm^{-1} are observed, which are caused by

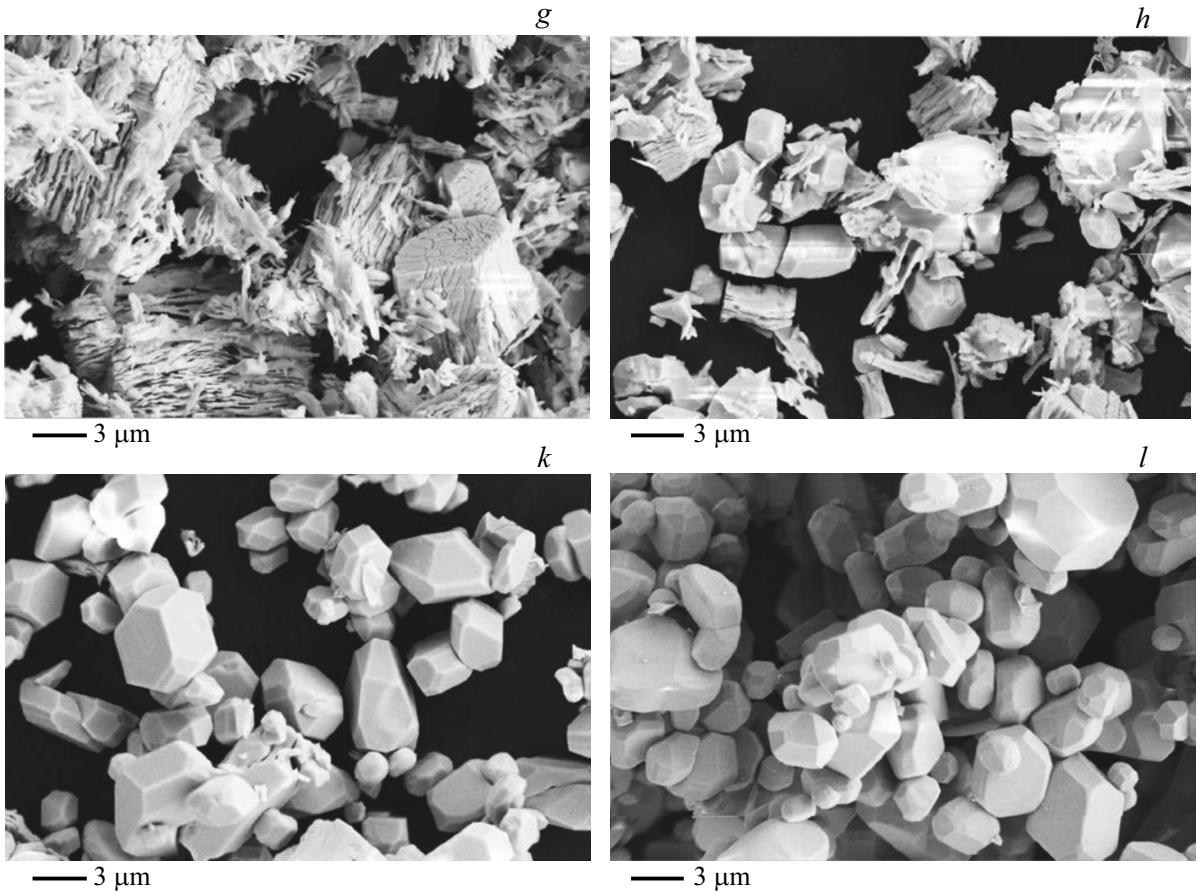

Fig. 5 (*continued*).

oscillations of B–O bonds in the structure with trigonal coordination of boron atoms, which is typical for the calcite phase (Fig. 6, spectrum *1*) [22,25,39]. In accordance with the analysis of internal vibrations of the $(BO_3)^{3-}$ ion in the structure of calcite [22], the IR-absorption band of 629 cm^{-1} can be attributed to the in-plane bending vibration ν_4, the doublet 747, 773 can be attributed to the out-of-plane bending vibration ν_2, and the absorption band of 1239 cm^{-1} can be attributed to antisymmetric stretching vibration ν_3 (Fig. 6, spectrum *1*). The spectrum of the sample with the composition of $Lu_{0.89}Sm_{0.1}Eu_{0.01}BO_3$ (Fig. 6, spectrum *2*) coincides with spectrum *1*, i.e. it contains the same set of absorption bands indicated as „c". According to the X-ray phase analysis data, the calcite phase in this sample is 100%.

With an increase in concentration of Sm^{3+}, additional bands „v" arise in the spectra of $Lu_{0.99-x}Sm_xEu_{0.01}BO_3$ ($0.2 \le x \le 0.25$) samples along with the calcite phase bands (Fig. 6, spectra *3, 4*). Their intensity increases with increase in the Sm^{3+} concentration, while intensity of bands of the calcite phase „c" decreases. According to the X-ray phase analysis results, $Lu_{0.79}Sm_{0.2}Eu_{0.01}BO_3$ and $Lu_{0.74}Sm_{0.25}Eu_{0.01}BO_3$ samples are two-phase samples with a calcite/vaterite ratio of 69/31 and 39/61%, respectively.

In the spectrum of the sample with the composition of $Lu_{0.69}Sm_{0.3}Eu_{0.01}BO_3$ (Fig. 6, spectrum *5*) only absorption bands indicated as „v" are observed: 572, 717, 879, 936, 1038, and 1082 cm^{-1}, which are typical for the vaterite phase with tetrahedral coordination of boron atoms [22,25]. As it was shown by the X-ray phase analysis, the $Lu_{0.69}Sm_{0.3}Eu_{0.01}BO_3$ sample is single-phase with a structure of vaterite (Table 2). Previously it was found that at concentrations of rare earth element greater than 15–20 at.%, $Lu_{1-x}Re_xBO_3$ compounds (Re = Eu, Tb, Gd, Dy, and Y) have a structure of vaterite [25]. A similar situation is observed in $Lu_{0.99-x}Sm_xEu_{0.01}BO_3$ compounds at $0.3 \le x \le 0.95$. IR-spectra of $Lu_{0.99-x}Sm_xEu_{0.01}BO_3$ samples at $0.3 \le x \le 0.95$ (Fig. 6, spectra *5–9*) contain only absorption bands typical for the vaterite phase „v". According to the X-ray phase analysis data (Table 2), these samples indeed have a vaterite structure. It should be noted, that in the range of existence of the vaterite phase ($0.3 \le x \le 0.95$), with an increase in x a shift toward low energies occurs of the absorption bands maxima caused by the oscillations of B–O bonds (Fig. 6, spectra *5–9*, dashed line). In the sample with the composition of $Lu_{0.04}Sm_{0.95}Eu_{0.01}BO_3$ absorption bands of 566, 690, 856, 914, 995, and 1041 cm^{-1} are observed. This shift is correlated with the increase in the lattice cell volume of

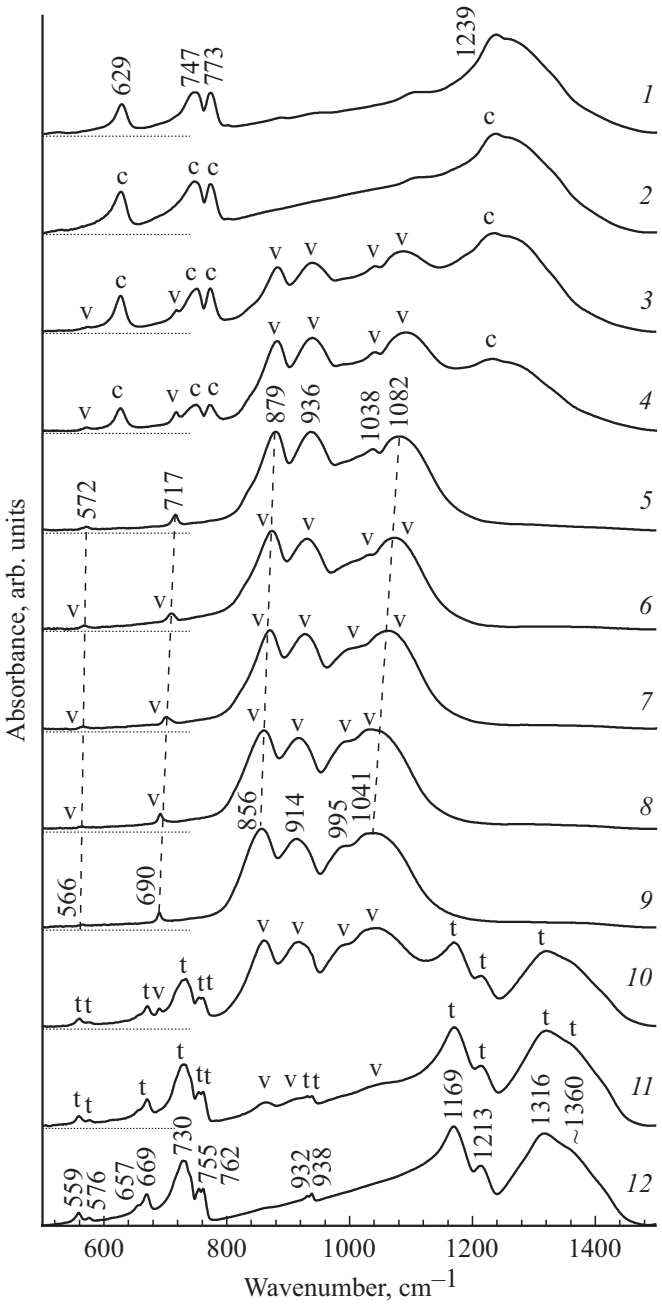

Figure 6. IR-spectra of orthoborates *1* — $Lu_{0.99}Eu_{0.01}BO_3$; *2* — $Lu_{0.89}Sm_{0.1}Eu_{0.01}BO_3$; *3* — $Lu_{0.79}Sm_{0.2}Eu_{0.01}BO_3$; *4* — $Lu_{0.74}Sm_{0.25}Eu_{0.01}BO_3$; *5* — $Lu_{0.69}Sm_{0.3}Eu_{0.01}BO_3$; *6* — $Lu_{0.49}Sm_{0.5}Eu_{0.01}BO_3$; *7* — $Lu_{0.29}Sm_{0.7}Eu_{0.01}BO_3$; *8* — $Lu_{0.09}Sm_{0.9}Eu_{0.01}BO_3$; *9* — $Lu_{0.05}Sm_{0.95}BO_3$; *10* — $Lu_{0.035}Sm_{0.965}BO_3$; *11* — $Lu_{0.02}Sm_{0.98}BO_3$; *12* — $SmBO_3$. For the spectra *1–11*, the zero values of the ordinate axes are shown by a dotted line. For the spectra *5–9*, dashed lines shows the shift of vaterite phase lines of $Lu_{0.99-x}Sm_xEu_{0.01}BO_3$ orthoborates with changes in concentration of samarium.

$Lu_{0.99-x}Sm_xEu_{0.01}BO_3$ orthoborates with an increase of x in the range of $0.3 \le x \le 0.95$ (Fig. 3).

In the spectrum of $Lu_{0.035}Sm_{0.965}BO_3$ sample absorption bands indicated as „t“ arise along with the bands typical for vaterite phase („v“). With an increase in concentration of Sm^{3+}, the intensity of vaterite phase bands decreases, while that of bands „t“ increases (Fig. 6, spectra *10, 11*). In the spectrum of $SmBO_3$ sample only bands „t“ are observed (Fig. 6, spectrum *12*). According to the X-ray phase analysis data, $Lu_{0.035}Sm_{0.965}BO_3$ and $Lu_{0.02}Sm_{0.98}BO_3$ samples contain vaterite phase and triclinic phase of $SmBO_3$ with a ratio of vaterite/triclinic phase of 44/56 and 9/91%, respectively, while the $SmBO_3$ sample is single-phase with a triclinic structure (Table 2). In the IR-spectrum of the $SmBO_3$ sample absorption bands of 559, 576, 657, 669, 730, 755, 762, 932, 938, 1169, 1213, 1316 with a shoulder of $\sim 1360\,cm^{-1}$ are observed (Fig. 6, spectrum *12*). The IR-spectrum of $SmBO_3$ obtained in this work is similar to the IR-spectrum obtained for the $SmBO_3$ sample with a triclinic structure (sp. gr. P-1) in [41].

Previously it was found that the low-temperature modification of $SmBO_3$, which is stable in the range from room temperature to $\sim 1100^\circ C$, has a triclinic structure where boron atoms have trigonal coordination (planar triangular groups of BO_3) [30,41]. In [20,23,31,32] an interpretation was given for the absorption bands caused by vibrations of B–O bonds in IR-spectra of orthoborate samples with a triclinic structure, according to which the absorption bands in the range of $1100-1400\,cm^{-1}$ and the band with maximum at $938\,cm^{-1}$ can be attributed to antisymmetric stretching vibrations and symmetric stretching vibrations, respectively, the absorption in the range of $710-780\,cm^{-1}$ can be attributed to out-of-plane bending vibrations, and bands in the range of $550-680\,cm^{-1}$ can be attributed to in-plane bending vibrations of B–O bonds.

The evolution of IR-spectra of samples in the range of oscillations of B–O bonds with increase in concentration of Sm^{3+} in the $Lu_{0.99-x}Sm_xEu_{0.01}BO_3$ ($0 \le x \le 0.99$) system is accompanied with a change in coordination of boron atoms in the following sequence: trigonal → trigonal + tetrahedral → tetrahedral → tetrahedral + trigonal → trigonal, that corresponds to the following change in their phase composition: calcite → calcite + vaterite → vaterite → vaterite + triclinic phase → triclinic phase.

Thus, an unambiguous correspondence is observed between IR-spectra and structure of $Lu_{0.99-x}Sm_xEu_{0.01}BO_3$ orthoborates at $0 \le x \le 0.99$.

6. Luminescence spectra and luminescence excitation spectra

In luminescence spectra of Eu^{3+} ions in samples of $LuBO_3(Eu)$ with a structure of calcite two narrow bands were observed with $\lambda_{max} = 589.8$ and 595.7 nm (electron transition $^5D_0 \to {}^7F_1$) [7,9,25]. The luminescence spectrum for Eu^{3+} ions in the vaterite modification of $ReBO_3(Eu)$, where $Re = (Lu, Tb, Y, Gd)$ contains three bands: in the wavelength region of 588–596 nm (elec-

tron transition $^5D_0 \rightarrow {}^7F_1$), 608–613 and 624–632 nm ($^5D_0 \rightarrow {}^7F_2$) [3,7,9,25,34].

As known, rare-earth ions — Re^{3+} (including Eu^{3+}) are sensitive to the closest environment [35,36]. Therefore, the change of spectral characteristics of Re^{3+} ions allows evaluating the change in their local environment. Eu^{3+} ions allow monitoring the structural state both in volume and on surface of a sample. The information on the closest environment of Eu^{3+} ions in the crystal volume can be obtained by exciting the luminescence of Eu^{3+} ions by light with an energy, corresponding to the resonance excitation of Eu^{3+} ions ($\lambda_{ex} \sim 394$ and ~ 466 nm, electron transitions $^7F_0 \rightarrow {}^5L_6$ and $^7F_0 \rightarrow {}^5D_2$, respectively), in the transparent region of samples ($\lambda > 300$ nm) [8,26,27]. Excitation of luminescence of Eu^{3+} rare-earth ions by light with an energy within the intense absorption region of a sample ($\lambda = 225–300$ nm), the charge transfer band (CTB), allows obtaining the information on local environment of Eu^{3+} ions in the near-surface crystal layer [8,26,27]. In [36–39] it is shown, that if the closest order around Eu^{3+} ions is the same for the whole sample, that is indicated by coincidence of luminescence spectra (LS) of the near-surface sample layer and the sample volume, the sample is single-phase.

6.1. Luminescence spectra of $Lu_{0.99-x}Sm_xEu_{0.01}BO_3$ orthoborates

Fig. 7 shows luminescence spectra (LS) of $Lu_{0.99-x}Sm_xEu_{0.01}BO_3$ ($x = 0, 0.1, 0.2, 0.25$ and 0.3) compounds under excitation with the light corresponding to the resonance excitation of Eu^{3+} ions ($\lambda_{ex} = 394$ nm), and in the maximum of the charge transfer band ($\lambda_{ex} \sim 250–230$ nm). It should be noted that with increase in concentration of Sm^{3+} the luminescence intensity of $Lu_{0.99-x}Sm_xEu_{0.01}BO_3$ samples decreases and at $x > 0.3$ no luminescence is observed. The luminescence spectra of the near-surface layer ($\lambda_{ex} = 250$ nm) and the volume ($\lambda_{ex} = 394$ nm) of samples that contain 0 and 10 at.% of Sm^{3+} are the same (Fig. 7, spectra *1–4*). They contain bands with $\lambda_{max} = 589.8$ and 595.7 nm ($^5D_0 \rightarrow {}^7F_1$) typical for the calcite modification of $LuBO_3$(Eu). According to the X-ray phase analysis data, the $Lu_{0.99-x}Sm_xEu_{0.01}BO_3$ compound at $0 \le x \le 0.1$ indeed has a calcite structure (Table 2). In luminescence spectrum (LS) of the near-surface layer of the sample containing 20 at.% of Sm^{3+} bands with $\lambda_{max} = 589.8$ and 595.7 nm typical for the calcite modification are observed (Fig. 7, spectrum *5*). At the same time the LS of volume of this sample predominantly contains bands with $\lambda_{max} \sim 592.5$, ~ 611 and 628 nm (Fig. 7, spectrum *6*), which are typical for the vaterite modification of $LuBO_3$(Eu). The presence of calcite phase among others in the volume of the sample is indicated by the presence of a band with $\lambda_{max} = 589.8$ nm in the LS (Fig. 7, spectrum *6*). According to the X-ray phase analysis data, the $Lu_{0.79}Sm_{0.2}Eu_{0.01}BO_3$ orthoborate contains 69% of calcite and 31% of vaterite (Table 2). The occurrence of bands ($\lambda_{ex} = 394$ nm) corresponding to vaterite structure in the volumetric LS of the sample is indicative of the fact that the vaterite phase is formed first in the volume of $Lu_{0.99-x}Sm_xEu_{0.01}BO_3$ orthoborates. In the luminescence spectrum of near-surface layer of the $Lu_{0.74}Sm_{0.25}Eu_{0.01}BO_3$ compound the most intensive are the bands that correspond to the calcite modification of $LuBO_3$(Eu) — 589.8 and 595.7 nm (Fig. 7, spectrum *7*). In addition to these bands, in the LS spectrum of the sample that contains 25 at.% of Sm, a weak band in the wavelength range of 600–635 nm is observed. In the luminescence spectrum of volume of this sample, only the bands that correspond to vaterite phase are observed: ~ 592.5, 611, and 628 nm (Fig. 7, spectrum *8*). The $Lu_{0.74}Sm_{0.25}Eu_{0.01}BO_3$ orthoborate contains 31% of calcite and 69% of vaterite (Table 2). In the luminescence spectrum of near-surface layer of the $Lu_{0.69}Sm_{0.3}Eu_{0.01}BO_3$ compound, which has a vaterite structure according to the X-ray phase analysis data (Table 2), a very weak luminescence is observed without clearly distinguished maxima (Fig. 7, spectrum *9*). The luminescence spectrum of volume of the $Lu_{0.69}Sm_{0.3}Eu_{0.01}BO_3$ sample contains only the bands typical to the vaterite phase: 588–596 nm ($\lambda_{max} \sim 592.5$ nm), 608–613, and 624–632 nm ($\lambda_{max} \sim 611$ and 628 nm) (Fig. 7, spectrum *10*).

Thus, based of the investigation of luminescence spectra of the near-surface layer and volume of samples, a conclusion can be made that with an increase in concentration of Sm^{3+} ions in $Lu_{0.99-x}Sm_xEu_{0.01}BO_3$ orthoborates the vaterite phase occurs first in the volume of microcrystals that have a structure of calcite, as well as in the $Lu_{0.99-x}Re_xEu_{0.01}BO_3$ samples (Re = Eu, Gd, Tb, Y) synthesized at 970°C [26,27].

6.2. Luminescence excitation spectra of $Lu_{0.99-x}Sm_xEu_{0.01}BO_3$ orthoborates

Luminescence excitation spectra (LES) of the most intensive luminescence bands of $Lu_{0.99-x}Sm_xEu_{0.01}BO_3$ orthoborates at $x = 0$, 0.1, 0.2, 0.25, and 0.3 are shown in Fig. 8. LES of the most intensive luminescence band ($\lambda_{max} = 589.8$ nm) of $Lu_{0.99}Eu_{0.01}BO_3$ and $Lu_{0.89}Sm_{0.1}Eu_{0.01}BO_3$ compounds contain an intensive short-wave band ($\lambda_{max} \sim 250$ nm) (the charge transfer band — CTB) and weak resonance bands of the Eu^{3+} ion — 394 nm ($^7F_0 \rightarrow {}^5L_6$) and 466–470 nm ($^7F_0 \rightarrow {}^5D_2$) (Fig. 8, spectra *1, 2*). The intensity of the short-wave band ($\lambda_{max} \sim 250$ nm) is more than 35 times higher than that of the most intensive resonance band ($\lambda_{max} = 394$ nm). This LES is typical for the calcite modification of $LuBO_3$(Eu) [2,3,7,9,25]. According to the X-ray phase analysis data, these samples have a calcite structure (Table 2). In $Lu_{0.79}Sm_{0.2}Eu_{0.01}BO_3$ samples that contain 69% of calcite (C) and 31% of vaterite (V), the luminescence excitation spectrum of the most intensive luminescence band in the luminescence spectrum of the near-surface layer ($\lambda_{max} = 589.8$ nm) contains a band with $\lambda_{max} \sim 250$ nm

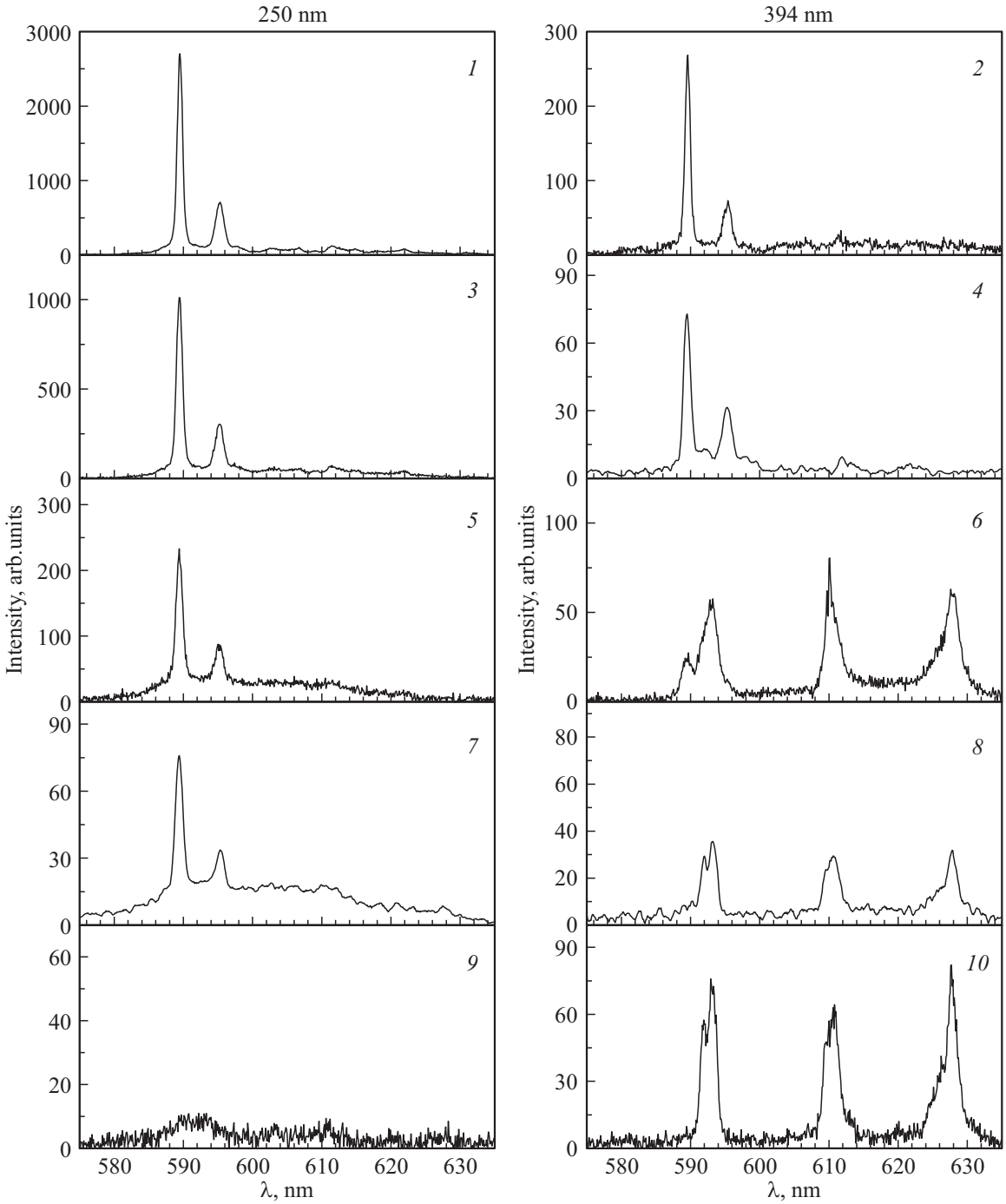

Figure 7. Luminescence spectra of orthoborates. $Lu_{0.99-x}Sm_xEu_{0.01}BO_3$ *1, 2* — $Lu_{0.99}Eu_{0.01}BO_3$; *3, 4* — $Lu_{0.89}Sm_{0.1}Eu_{0.01}BO_3$; *5, 6* — $Lu_{0.79}Sm_{0.2}Eu_{0.01}BO_3$; *7, 8* — $Lu_{0.74}Sm_{0.25}Eu_{0.01}BO_3$; *9, 10* — $Lu_{0.69}Sm_{0.3}Eu_{0.01}BO_3$. *1, 3, 5, 7, 9* — $\lambda_{ex} = 250$ nm; *2, 4, 6, 8, 10* — $\lambda_{ex} = 394$ nm.

and weak resonance bands of the Eu^{3+} ion (Fig. 8, spectrum *3*). At the same time, the LES of the most intensive luminescence band in the LS of volume of this sample ($\lambda_{max} = 611$ nm) (Fig. 7, spectrum *6*) contains a wide ultraviolet band (CTB) ($\lambda_{max} \sim 240-260$ nm) and resonance bands at 394 and 466–470 nm. The intensity of the 394 nm band is about 5 times less than the CTB intensity (Fig. 8, spectrum *4*). The LES of the most intensive luminescence band ($\lambda_{max} = 589.8$ nm) in the LS of volume of the $Lu_{0.74}Sm_{0.25}Eu_{0.01}BO_3$ (31% of C and 69% of V) contains a CTB ($\lambda_{max} \sim 250$ nm) and very weak resonance bands of the Eu^{3+} ion (Fig. 8, spectrum *5*). LES of the most intensive luminescence band of volume of this sample ($\lambda_{max} = 611$ nm) is similar to LES of the sample that contains 20 at.% of Sm (Fig. 8, spectra *4, 6*). In the luminescence excitation spectrum of the most intensive lumines-

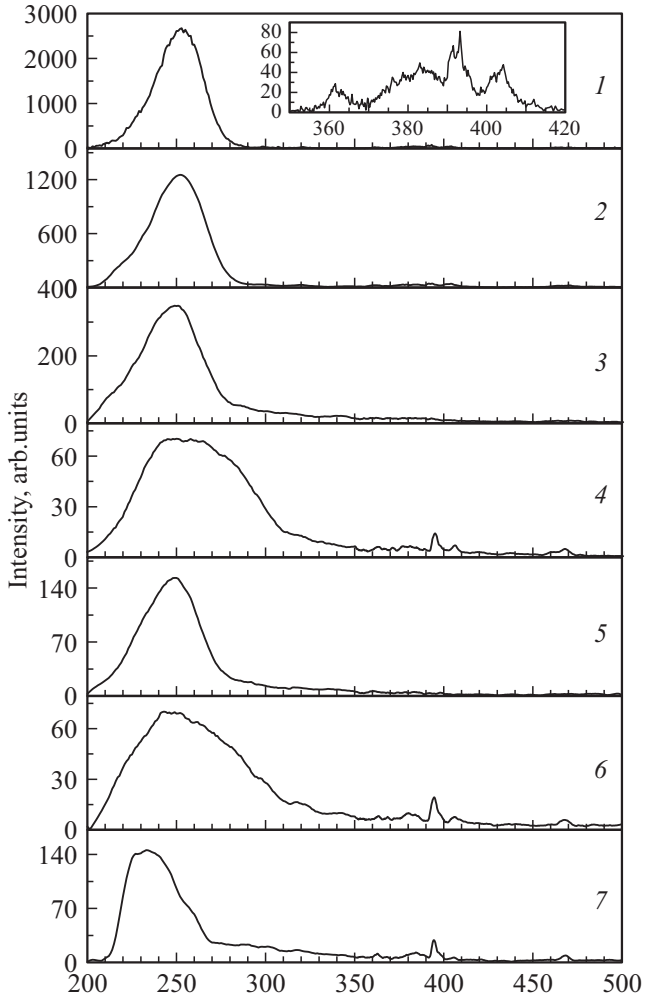

Figure 8. Luminescence excitation spectra of orthoborates $Lu_{0.99-x}Sm_xEu_{0.01}BO_3$ *1* — $Lu_{0.99}Eu_{0.01}BO_3$; *2* — $Lu_{0.89}Sm_{0.1}Eu_{0.01}BO_3$; *3* — $Lu_{0.79}Sm_{0.2}Eu_{0.01}BO_3$; *4* — $Lu_{0.79}Sm_{0.2}Eu_{0.01}BO_3$; *5* — $Lu_{0.74}Sm_{0.25}Eu_{0.01}BO_3$; *6* — $Lu_{0.74}Sm_{0.25}Eu_{0.01}BO_3$; *7* — $Lu_{0.69}Sm_{0.3}Eu_{0.01}BO_3$. *1, 2, 3, 5* — $\lambda_{max} = 589.8$ nm; *4, 6* — $\lambda_{max} = 611$ nm; *7* — $\lambda_{max} = 592.5$ nm. The insert shows a zoomed in fragment of the spectrum in the range of 350–420 nm.

cence band ($\lambda_{max} = 592.5$ nm) of the $Lu_{0.69}Sm_{0.3}Eu_{0.01}BO_3$ sample (100% V) a band with $\lambda_{max} \sim 235$ nm is observed together with 394 and 466–470 nm bands. The intensity of the 394 nm band is ~ 4 times less than the CTB intensity. It is important to note, that while in the calcite modification of $Lu_{0.99-x}Sm_xEu_{0.01}BO_3$ orthoborates the CTB intensity is ~ 35 times higher than the intensity of the 394 nm band, in the compounds with a structure of vaterite this ratio is considerably lower (~ 4), which is typical for LES of orthoborates with a structure of vaterite [3,9,25].

Thus, based on the investigation of spectral characteristics of $Lu_{0.99-x}Sm_xEu_{0.01}BO_3$ orthoborates at $0 \le x \le 0.3$, a conclusion can be made that in this range of concentrations of Sm^{3+} a correspondence is observed between spectral characteristics and structure of these compounds. Based on the investigation of the luminescence spectra, a conclusion can be made that the vaterite phase occurs at ($x \ge 0.2$) in the volume of microcrystals of $Lu_{0.99-x}Sm_xEu_{0.01}BO_3$, that have a structure of calcite.

7. Conclusion

In this work we performed studies of structure, morphology, IR-spectra, and luminescence spectra of $Lu_{0.99-x}Sm_xEu_{0.01}BO_3$ orthoborates at $0 \le x \le 0.99$ synthesized at 970°C.

We have found an unambiguous correspondence between the structural modification and IR spectra of these compounds. The investigation of luminescence spectra at different wavelengths of the exciting light has shown that the vaterite phase occurs at ($x \ge 0.2$) in the volume of microcrystals of $Lu_{0.99-x}Sm_xEu_{0.01}BO_3$, that have a structure of calcite. With increase in concentration of Sm^{3+} the luminescence intensity of $Lu_{0.99-x}Sm_xEu_{0.01}BO_3$ samples decreases and at $x > 0.3$ no luminescence is observed.

In $Lu_{0.99-x}Sm_xEu_{0.01}BO_3$ orthoborates synthesized at 970°C, with increase in concentration of samarium a successive change of three types of crystal structures takes place: calcite, vaterite, and triclinic phase.

At $0 \le x \le 0.1$ $Lu_{0.99-x}Sm_xEu_{0.01}BO_3$ orthoborates are single-phase with a structure of calcite (sp.gr. $R\bar{3}c$). In IR-spectra absorption bands at 629, 746, 773, and 1236 cm^{-1} are observed that correspond to the $LuBO_3$ calcite phase. The luminescence spectra contain bands with $\lambda_{max} = 589.8$ and 595.7 nm ($^5D_0 \rightarrow {}^7F_1$) typical for the calcite modification of $LuBO_3$(Eu).

At $0.1 < x < 0.3$ the samples are double-phase: they contain calcite and vaterite phases. In the IR-spectra and in luminescence spectra bands are observed, which are typical for calcite and vaterite structures.

At $0.3 \le x \le 0.95$ the $Lu_{0.99-x}Sm_xEu_{0.01}BO_3$ compounds become single-phase with a vaterite structure (sp.gr. $P6_3/mmc$). At $x = 0.3$ in the IR-spectra the absorption bands of vaterite phase are observed: 572, 717, 879, 936, 1038, and 1082 cm^{-1}. With increase in concentration of Sm^{3+} ions, a shift of these bands is observed toward the low-energy region, which correlates with the increase in parameters of the lattice cell. At $x = 0.95$ maxima of IR-absorption bands are observed at 566, 690, 856, 914, 995, and 1041 cm^{-1}. In luminescence spectra of $Lu_{0.69}Sm_{0.3}Eu_{0.01}BO_3$ samples only the bands with $\lambda_{max} = 592.5$ nm ($^5D_0 \rightarrow {}^7F_1$), 611, and 628 nm ($^5D_0 \rightarrow {}^7F_2$) are observed, which are typical for the vaterite structure.

At $0.95 < x \le 0.98$ samples of $Lu_{1-x}Sm_xBO_3$ are double-phase. They contain the triclinic phase of $SmBO_3$ along with vaterite. The IR-spectra have the bands typical for the vaterite and triclinic modifications of these samples.

At $0.98 < x \le 1$ samples of $Lu_{1-x}Sm_xBO_3$ are single-phase with a triclinic structure (sp.gr. $P(\bar{1})$). In the

IR-spectra of these samples absorption bands in frequency ranges of $1100-1400\,cm^{-1}$, $710-780\,cm^{-1}$, $550-680\,cm^{-1}$, and near $938\,cm^{-1}$ are observed that correspond to the triclinic phase of $SmBO_3$.

The range of Sm^{3+} concentrations where the vaterite phase exists in $Lu_{0.99-x}Sm_xEu_{0.01}BO_3$ orthoborates synthesized at 970°C is very wide: $0.3 \le x \le 0.95$, at the same time, the triclinic phase exists in a very narrow range: $0.98 < x \le 1$.

Thus, in $Lu_{0.99-x}Sm_xEu_{0.01}BO_3$ orthoborates synthesized at $T = 970$°C (the temperature of existence of the $LuBO_3$ calcite phase and the $SmBO_3$ triclinic phase), with an increase in Sm^{3+} concentration a successive change of five structural states is observed: calcite $(0 \le x \le 0.1) \rightarrow$ calcite + vaterite $(0.1 < x < 0.3) \rightarrow$ vaterite $(0.3 \le x \le 0.95) \rightarrow$ vaterite + triclinic phase $(0.95 < x \le 0.98) \rightarrow$ triclinic phase $(0.98 < x \le 1)$.

Acknowledgments

The authors thank the Research Facility Center of ISSP RAS for the morphology study of the samples and their characterization by IR-spectroscopy and X-ray phase analysis methods.

Funding

The research is carried out within the state task of ISSP RAS.

Conflict of interest

The authors declare that they have no conflict of interest.

References

[1] E.F. Shubert, J.K. Kim. Science **308**, 1274 (2005).
[2] X. Zhang, X. Fu, J. Song, M.-L. Gong. Mater. Res. Bull. **80**, 177 (2016).
[3] C. Mansuy, J.M. Nedelec, C. Dujardin, R. Mahiou. Opt. Mater. **29**, 697 (2007)
[4] A.B. Kuznetsov, K.A. Kokh, N.G. Kononova, V.S. Shevchenko, S.V. Rashchenko, D.M. Ezhov, A.Y. Jamous, A. Bolatov, B. Uralbekov, V.A. Svetlichnyi, A.E. Kok. J. Alloys Comp. **851**, 156825 (2021).
[5] V.V. Mikhailin, D.A. Spassky, V.N. Kolobanov, A.A. Meotishvili, D.G. Permenov, B.I. Zadneprovski. Rad. Measurem. **45**, 307 (2010).
[6] G. Blasse, B.C. Grabmaier. Luminescent Materials. Berlin–Heiderberg: Springer–Verlag (1994). 233 p.
[7] Jun Yang, Chunxia Li, Xiaoming Zhang, Zewei Quan, Cuimiao Zhang, Huaiyong Li, Jun Lin. Chem. Eur. J. **14**, *14*, 4336 (2008).
[8] S.Z. Shmurak, V.V. Kedrov, A.P. Kiselev, T.N. Fursova, I.I. Zver'kova, FTT **62**, *12*, 2110 (2020) (in Russian).
[9] S.Z. Shmurak, V.V. Kedrov, A.P. Kiselev, I.M. Shmyt'ko, FTT **57**, *1*, 19 (2015) (in Russian).
[10] E.M. Levin, R.S. Roth, J.B. Martin. Am. Miner. **46**, *9–10*, 1030 (1961).
[11] J. Hölsä. Inorg. Chim. Acta **139**, *1–2*, 257 (1987).
[12] G. Chadeyron, M. El-Ghozzi, R. Mahiou, A. Arbus, C. Cousseins. J. Solid State Chem. **128**, 261 (1997).
[13] D. Santamaría-Pérez, O. Gomis, J. Angel Sans, H.M. Ortiz, A. Vegas, D. Errandonea, J. Ruiz-Fuertes, D. Martinez-Garcia, B. Garcia-Domene, André L.J. Pereira, F. Javier Manjón, P. Rodríguez-Hernández, A. Muñoz, F. Piccinelli, M. Bettinelli, C. Popescu. J. Phys. Chem. C **118**, 4354 (2014).
[14] Wen Ding, Pan Liang, Zhi-Hong Liu. Mater. Res. Bull. **94**, 31 (2017).
[15] Wen Ding, Pan Liang, Zhi-Hong Liu. Solid State Sci. **67**, 76 (2017).
[16] Heng-Wei Wei, Li-Ming Shao, Huan Jiao, Xi-Ping Jing. Opt. Mater. **75**, 442 (2018).
[17] R. Nayar, S. Tamboli, A.K. Sahu, V. Nayar, S.J. Dhoble. J. Fluoresc. **27**, 251 (2017).
[18] S.K. Omanwar, N.S. Savala. Appl. Phys. A **123**, 673 (2017).
[19] A. Haberer, R. Kaindl, H. Huppertz. Z. Naturforsch. B **65**, 1206 (2010).
[20] R. Velchuri, B.V. Kumar, V.R. Devi, G. Prasad, D.J. Prakash, M. Vital. Mater. Res. Bull. **46**, *8*, 1219 (2011).
[21] Jin Teng-Teng, Zhang Zhi-Jun, Zhang Hui, Zhao Jing-Tai. J. Inorgan. Mater. **28**, *10*, 1153 (2013).
[22] C.E. Weir, E.R. Lippincott. J. RES. Natl. Bur. Std.-A. Phys. Chem. **65A**, *3*, 173 (1961).
[23] A. Szczeszak, T. Grzyb, St. Lis, R.J. Wiglusz. Dalton Transact. **41**, 5824 (2012).
[24] Ling Li, Shihong Zhou, Siyuan Zhang. Solid State Sci. **10**, 1173 (2008).
[25] S.Z. Shmurak, V.V. Kedrov, A.P. Kiselev, T.N. Fursova, I.M. Shmytko. FTT **57**, *8*, 1558 (2015) (in Russian).
[26] S.Z. Shmurak, V.V. Kedrov, A.P. Kiselev, T.N. Fursova, I.I. Zver'kova, E.Yu. Postnova, FTT **63**, *7*, 933 (2021) (in Russian).
[27] S.Z. Shmurak, V.V. Kedrov, A.P. Kiselev, T.N. Fursova, I.I. Zver'kova, E.Yu. Postnova, FTT **63**, *10*, 1617 (2021) (in Russian).
[28] S.Z. Shmurak, V.V. Kedrov, A.P. Kiselev, T.N. Fursova, I.I. Zver'kova, S.S. Khasanov, FTT **63**, *12*, 2142 (2021) (in Russian).
[29] S.Z. Shmurak, V.V. Kedrov, A.P. Kiselev, T.N. Fursova, I.I. Zver'kova, FTT **64**, *4*, 474 (2022) (in Russian).
[30] K.K. Palkina, V.G. Kuznetsov, L.A. Butman, B.F. Dzhurinsky, Koordinatsionnaya khimiya **2**, *2*, 286 (1976) (in Russian).
[31] S. Lemanceau, G. Bertrand-Chadeyron, R. Mahiou, M. El-Ghozzi, J.C. Cousseins, P. Conflant, R.N. Vannier. J. Solid State Chem. **148**, 229 (1999).
[32] N. Akçamlı, D. Ağaoğulları, Ö. Balcı, M. Lütfi Öveçoğlu, I. Duman. Ceram. Int. **42**, 10045 (2016).
[33] A.G. Ryabukhin, Izv. Chelyabinsk. nauch. tsentra **4**, 33 (2000) (in Russian).
[34] J. Yang, G. Zhang, L. Wang, Z. You, S. Huang, H. Lian, J. Lin. J. Solid State Chem. **181**, *12*, 2672 (2008).
[35] M.A. Elyashevich, Spektroskopiya redkikh zemel', GITTL, M. (1953). 456 p. (in Russian).
[36] M.I. Gaiduk, V.F. Zolin, L.S. Gaigerova. Spektry lyuminestsentsii evropiya. Nauka, M. (1974), 195 p. (in Russian).
[37] S.Z. Shmurak, A.P. Kiselev, V.V. Sinitsyn, I.M. Shmyt'ko, A.S. Aronin, B.S. Red'kin, E.G. Ponyatovsky, FTT **48**, *1*, 48 (2006) (in Russian).

[38] S.Z. Shmurak, A.P. Kiselev, N.V. Klassen, V.V. Sinitsyn, I.M. Shmyt'ko, B.S. Red'kin, S.S. Khasanov. IEEE Trans. Nucl. Sci. **55**, *1–3*, 1128 (2008).
[39] S.Z. Shmurak, A.P. Kiselev, D.M. Kurmasheva, B.S. Red'kin, V.V. Sinitsyn, ZhETF **137**, *5*, 867 (2010) (in Russian).
[40] D. Boyer, F. Leroux, G. Bertrand, R. Mahiou. J. Non-Crystalline Solids **306**, *2*, 110 (2002).
[41] https://open.metu.edu.tr/bitstream/handle/11511/18903/index.pdf
[42] G. Corbel, M. Leblanc, E. Abtic-Fidancev, M. Lemaitre-Blaise, J.C. Krupa. J. Alloys Comp. **287**, 71–78 (1999),

Translated by Ego Translating